Available online at www.sciencedirect.com
ScienceDirect
Phytochemistry 68 (2007) 2523–2530
PHYTOCHEMISTRY
www.elsevier.com/locate/phytochem

Biotransformation of 20(*S*)-protopanaxatriol by *Mucor spinosus* and the cytotoxic structure activity relationships of the transformed products

Jie Zhang [a], Hongzhu Guo [a,b,*], Yin Tian [a], Peng Liu [a], Na Li [b], Jianping Zhou [b], Dean Guo [a,c,*]

[a] *Division of Pharmacognostical Biotechnology, School of Pharmaceutical Sciences, Peking University, Beijing 100083, China*
[b] *Beijing Institute for Drug Control, Beijing 100035, China*
[c] *The State Key Laboratory of Natural and Biomimetic Drugs, School of Pharmaceutical Sciences, Peking University, Beijing 100083, China*

Received 16 October 2006; received in revised form 26 March 2007
Available online 10 July 2007

Abstract

Biotransformation of 20(*S*)-protopanaxatriol (**1**) by the fungus *Mucor spinosus* AS 3.3450 gave 10 metabolites (**2**–**10**), of which **2**–**5** were previously known. On the basis of NMR and MS analyses, structures **6**–**10** were established as 12-oxo-23β-hydroxyl-20(*S*)-protopanaxatriol (**6**), 20*S*,24*R*-epoxy-dammaran-3β,6α,25-triol-12-one (**7**), 29-hydroxyl-20(*S*)-protopanaxatriol (**8a**), 12-oxo-11β-hydroxyl-20(*S*)-protopanaxatriol (**8b**), 28-hydroxyl-20(*S*)-protopanaxatriol (**9**) and 12-oxo-20(*S*)-protopanaxatriol (**10**). The biotransformation kinetics of **1** has been investigated and a possible biotransformation pathway proposed. The *in vitro* cytotoxic activities of metabolites against three human cancer cell lines were determined by the MTT method; compounds **8a**, **9** and **10** had more potent inhibitory effects against HL-60 cell line than the substrate.

Keywords: 20(*S*)-Protopanaxatriol; Biotransformation; *Mucor spinosus* AS 3.3450; Cytotoxic activity

1. Introduction

Ginsenosides are the main effective constituents isolated from the traditional Chinese herb ginseng, the roots of *Panax ginseng* C.A. Meyer. Many of these compounds have significant antitumor activities (Shibata, 2001), which are mediated by inhibition of tumor-induced angiogenesis (Sato et al., 1994), tumor invasion and metastasis (Mochizuki et al., 1995; Shinkai et al., 1996). Research has found that the intestinal bacterial metabolites of ginsenosides are responsible for the main pharmacological activities of ginseng (Bae et al., 2002; Liu et al., 2004; Wakabayashi et al., 1997). For example, Rg1 was converted to 20(*S*)-protopanaxatriol (**1**) via ginsenoside Rh1 by human intestinal bacteria after oral administration (Shibata, 2001). 20(*S*)-Protopanaxatriol (**1**) is the main bacterial metabolite of protopanaxatriol-type ginsenosides and has been reported to mediate their antitumor effects (Hasegawa et al., 2002). *In vitro* cytotoxic experiments have shown that the aglycone 20(*S*)-protopanaxatriol (**1**) reduces cell proliferation in human leukemia THP-1 cells (Popovich and Kitts, 2002) and two intestinal cell lines, Int-407 and Caco-2 (Popovich and Kitts, 2004). It can also enhance the effects of chemotherapeutics on multi-drug resistant (MDR) cancer cell lines (Hasegawa et al., 1995) and the cytotoxicities of other anticancer drugs in adriamycin (ADM)-resistant P388 leukemia cells (Atopkina et al., 1999). Animal experiments with C57BL/6 mice implanted with B16-BL6 melanoma showed that chronic oral administration of 20(*S*)-protopanaxatriol (**1**) inhibited the growth of B16-BL6 melanoma at the implanted site (Hasegawa et al.,

* Corresponding authors. Address: Division of Pharmacognostical Biotechnology, School of Pharmaceutical Sciences, Peking University, Beijing 100083, China. Tel./fax: +86 10 82805107 (H. Guo); tel./fax: +86 10 82802700 (D. Guo).
E-mail addresses: guohz@bjmu.edu.cn (H. Guo), gda@bjmu.edu.cn (D. Guo).

0031-9422/$ - see front matter © 2007 Elsevier Ltd. All rights reserved.
doi:10.1016/j.phytochem.2007.05.028

2002). Investigation of the mechanisms of antitumor activities of 20(*S*)-protopanaxatriol (**1**) showed that it did not inhibit tumor growth *in vivo* directly, but that it stimulated splenic NK cells to become cytotoxic to tumor cells (Hasegawa et al., 2002). Thus, 20(*S*)-protopanaxatriol (**1**) has attracted much attention recently.

Biotransformation is considered to be an economically and ecologically viable technology and has recently been used to modify the structures of some biologically active products and study the metabolism of natural products. Some of the fungal biotransformation products could be similar to those in humans due to the similarity between these two metabolic systems (de Carvalho and da Fonseca, 2006). Therefore, it can be a useful tool to mimic mammalian metabolism *in vitro* and obtain metabolites that are valuable for *in vivo* metabolism research.

The fungus *Mucor spinosus* AS 3.3450 was incubated with 20(*S*)-protopanaxatriol (**1**) to obtain various structurally modified derivatives with enhanced activity and improved bioavailability. The cytotoxicities of the metabolites on human tumor cell lines, including BGC-823, HeLa and HL-60 cells, were measured and the preliminary structure activity relationships were discussed.

2. Results and discussion

The substrate 20(*S*)-protopanaxatriol (**1**) was obtained from the ginsenoside extract by Smith's degradation method (Nagai et al., 1972). Twenty-one strains of fungi were screened for their abilities to metabolize **1**, of which *M. spinosus* AS 3.3450 was found to produce more diverse products with high efficiencies and was selected for preparative-scale biotransformation. Ten metabolites (**2**–**10**) were obtained when the substrate (**1**) was administered to the fungus (Fig. 1), of which compounds **6**–**10** were new compounds, whereas **2**–**5** have been reported previously (Tian et al., 2005).

HR-ESI-MS analysis of compound **6** gave a molecular formula of $C_{30}H_{50}O_5$. The ^{13}C NMR spectrum showed one new carbonyl signal at δ 211.6 and one new oxygen-bearing CH resonance at δ 66.2, compared with that of **1**, indicating that **6** was a hydroxylated and oxidized product. The position of the carbonyl group (C-12) was established based on HMBC correlations between it and H-11 (δ 2.37, *dd*, $J = 4.5$, 13 Hz), H-13 (δ 3.31, *d*, $J = 9.5$ Hz), H-17 (δ 2.63) and the chemical shift of C-11 and C-13. Correlation between δ 66.2 and H-22 in the HMBC spectrum indicated that the hydroxyl group was at C-23. The enhancements between 23-OH (δ 6.53) and 20-OH (δ 5.81), H-23 (δ 5.12) and 21-CH_3 (δ 1.56) in the NOESY spectrum suggested a β-configuration for 23-OH. Therefore, **6** was identified as 12-oxo-23β-hydroxyl-20(*S*)-protopanaxatriol.

Compound **7** had a molecular formula of $C_{30}H_{50}O_5$ (HR-ESI-MS). The ^{13}C NMR spectrum showed an additional carbonyl signal at δ 210.4, the long-range correlation

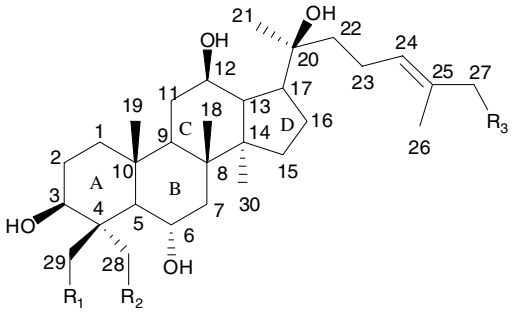

1 R_1=R_2=R_3=H
3 R_1=R_2=H, R_3=OH
8a R_1=OH, R_2=R_3=H
9 R_1=R_3=H, R_2=OH

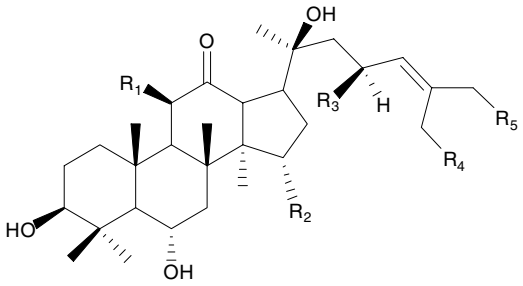

2 R_1=R_3=R_4=R_5=H, R_2=OH
4 R_1=R_2=R_3=R_5=H, R_4=OH
5 R_1= R_2=R_3=R_4=H, R_5=OH
6 R_1=R_2=R_4=R_5=H, R_3=OH
8b R_1=OH, R_2=R_3=R_4=R_5=H
10 R_1=R_2=R_3=R_4=R_5=H

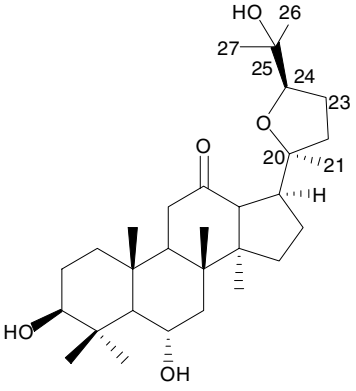

7

Fig. 1. Chemical structures of compounds **1**–**10**.

between it and H-17 (δ 2.72) in the HMBC spectrum and the chemical shift of C-11 and C-13 enabled it to be assigned to C-12. When further compared with **1**, significant differences were in the carbon signals from C-20–C-27, and the side-chain double bond (C_{24}–C_{25}) in **1** was replaced with a new oxygenated quaternary resonance (δ 71.1) and a new oxygenated tertiary signal (δ 84.6). The C-20 resonated at a much lower field (δ 85.3) and NOE

enhancements were observed between 21-CH_3 (δ 1.21) and H-24 (δ 3.93), H-26 (δ 1.39), and H-27 (δ 1.35), indicating cyclization of the side-chain. The structure and stereochemistry of the side-chain was established by comparison of the ^{1}H NMR and ^{13}C NMR spectra of **7** with data reported in the literature. The carbon signals attributable to the cyclized side-chain were identical to those of neoalsoside G1 (Fujita et al., 1995a), indicating that **7** has a 20*S*,24*R*-epoxy ring structure. The *S* configuration of C-20 could be easily confirmed due to significant differences in the chemical shifts of C-17, C-20 and C-21 between 20(*S*)- and 20(*R*)-compounds (Asakawa et al., 1977; Duc et al., 1994; Fujita et al., 1995b). Comparison of the ^{13}C NMR spectrum of **7** with that of 20*S*,24*S*-epoxy-3β,25-dihydroxydammaran-12-one (Fujita et al., 1995b) showed a close similarity between most of the data, except for the C-20–C-27 data, and the NOE enhancement between 21-CH_3 and H-24 further established the *R* configuration of C-24. Thus, the structure of **7** was determined as 20*S*,24*R*-epoxy-dammaran-3β,6α,25-triol-12-one.

The HR-ESI-MS spectrum suggested a molecular formula of $C_{30}H_{52}O_5$ for both **8a** and **9**, indicating that monohydroxylation had occurred. Analysis of the ^{13}C NMR and DEPT spectra for **8a** showed that a methyl group (δ 16.4) had disappeared and was replaced by an oxygen-bearing CH_2 at δ 64.0. The HMBC correlations of this carbon with H-3 (δ 3.67), H-5 (δ 1.29) and 28-CH_3 (δ 2.12) allowed assignment of the hydroxyl group to C-29. The ^{13}C NMR and DEPT data of **9** were very similar to those of **8a** except that the new CH_2 signal appeared at δ 69.3 and the missing methyl group was at δ 31.9, suggested that the hydroxylation position was at C-28 instead of C-29. This assignment was confirmed by the HMBC correlations between H-28 (H-28a, δ 4.52, *d*, $J = 10.5$ Hz; H-28b, δ 4.41, *d*, $J = 10.5$ Hz) and C-3, C-4, C-5 and C-29. Therefore, **8a** and **9** were characterized as 29-hydroxyl-20(*S*)-protopanaxatriol and 28-hydroxyl-20(*S*)-protopanaxatriol, respectively.

The molecular formula of compound **8b** was $C_{30}H_{50}O_5$ (HR-ESI-MS). The ^{13}C NMR spectrum showed a new carbonyl signal at δ 211.7 and a new oxygenated methine signal at δ 77.5, indicating that **8b** was a hydroxylated and oxidized product of **1**. Oxidization also occurred at C-12 due to its correlations with H-11 (δ 4.75, *t*, $J = 3$ Hz), H-13 (δ 4.41, *d*, $J = 9.5$ Hz) and H-17 (δ 2.88) in the HMBC spectrum. Analysis of the HMBC data showed that hydroxylation had taken place at C-11, because its corresponding proton signal (δ 4.75) had correlations with C-8, C-9 and C-13. The ^{1}H NMR signals for 18- and 19-CH_3 had shifted downfield significantly due to their 1,3-*cis*-diaxial interactions with 11-OH, suggesting an axial position for 11-OH. The NOE enhancements of H-11 (δ 4.75) with H-9 (δ 1.69) and of 11-OH (δ 7.51) with 18-CH_3 (δ 1.90) and 19-CH_3 (δ 1.82) confirmed the β-configuration of 11-OH. From the above results, **8b** was determined as 12-oxo-11β-hydroxyl-20(*S*)-protopanaxatriol.

Compound **10** had a molecular formula of $C_{30}H_{50}O_4$, as shown by HR-ESI-MS analysis. The loss of two hydrogens compared with **1** indicated the presence of a carbonyl group, which was determined to be at C-12 due to the correlations between it (δ 211.7) and H-13 (δ 3.32, *d*, $J = 9.5$ Hz), H-17 (δ 2.70), H-11 (δ 2.38), and H-9 (δ 1.88) in the HMBC spectrum. Thus, **10** was determined as 12-oxo-20(*S*)-protopanaxatriol.

In an effort to determine the possible biotransformation pathway of 20(*S*)-protopanaxatriol by (**1**) *M. spinosus* AS 3.3450, the time course of the biotransformation was investigated (Figs. 2–4). Substrate **1** was almost completely metabolized within 72 h of administration. 12-Oxo-20(*S*)-protopanaxatriol (**10**) was the first metabolite, it formed within 3 h and the concentration peaked at 24 h, then decreased rapidly to a minimal concentration, indicating the formation of other secondary products. Accordingly, after 12 h, some new 12-oxo products **2**, **4**, **5**, **6**, **7** and **8b** were detected. Therefore, we concluded that **10** was an intermediate product in the biosynthetic pathway and that 12-carbonylation was the first reaction in the pathway. It was followed by hydroxylation at various sites to generate metabolites **2** and **8b**, which appeared after 6 h, and metabolites **4**, **5**, **6** and **7**, which appeared after 12 h. This indicated that the hydroxylation of ring C occurred more easily than hydroxylation of the side-chain. The level of

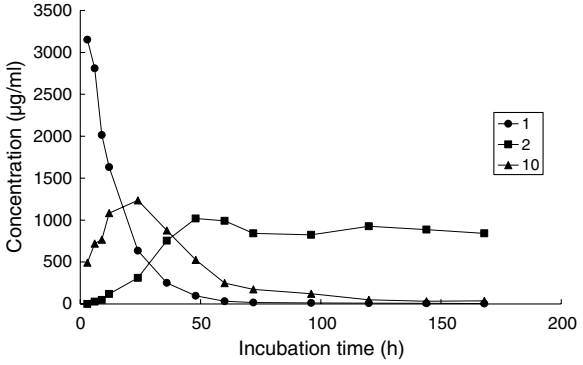

Fig. 2. Biotransformation kinetics of substrate **1** and metabolites **2** and **10**.

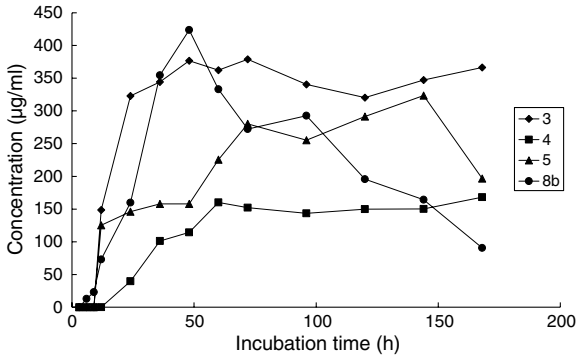

Fig. 3. Biotransformation kinetics of metabolites **3**, **4**, **5** and **8b**.

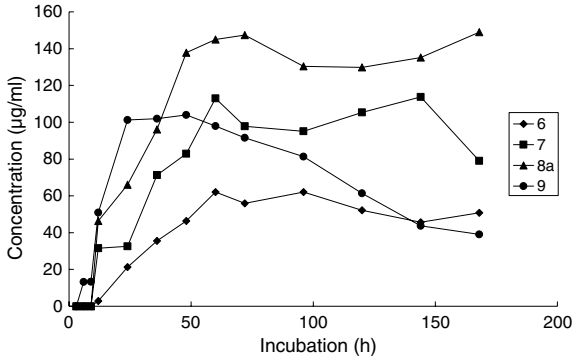

Fig. 4. Biotransformation kinetics of metabolites **6**, **7**, **8a** and **9**.

8b decreased gradually after peaking at 48 h, the concentration at 120 h was less than half of the maximum level, indicating that it might be converted back to **10** and then be metabolized to other products. Three monohydroxylated products, **3**, **8a** and **9**, were also observed after 6–12 h and maintained at a low level. After 100 h, the level of **8a** had increased gradually, whereas the level of **9** had decreased by a similar amount, indicating that **9** might be converted to **8a**. The same changes were observed between **3**, **4** and **5**. So, we propose a possible biotransformation pathway for the metabolism of 20(*S*)-protopanaxatriol (**1**) as shown in Fig. 5.

The cytotoxic activities of these products were evaluated with human gastric cancer BGC-823 cells, human cervical carcinoma HeLa cells and human leukemia HL-60 cells. All the metabolites and the substrate had very weak or no cytotoxic activities against BGC-823 and HeLa cells. The substrate **1** and metabolites **8a**, **9** and **10** had inhibitory effects against human leukemia HL-60 cells with IC50 values of 119.2, 83.3, 85.5 and 83.1 μM, respectively. The cytotoxic activities against human leukemia HL-60 cells were weak but some information could still be obtained. The metabolites **8a**, **9** and **10** had more potent cytotoxicities than the substrate **1**, indicating that hydroxylation at C-28 or C-29 and 12-carbonylation could increase the cytotoxicities. The hydroxylation at C-11β, C-15α, C-23β, C-26 and C-27 would significantly reduce the activities, and the corresponding compounds **8b**, **2**, **6**, **3**, **4** and **5** exhibited very weak or no cytotoxic effects. The cyclized product **7** had no effect on the bioassay, indicating that cyclization of the side-chain would markedly reduce the activity of the substrate.

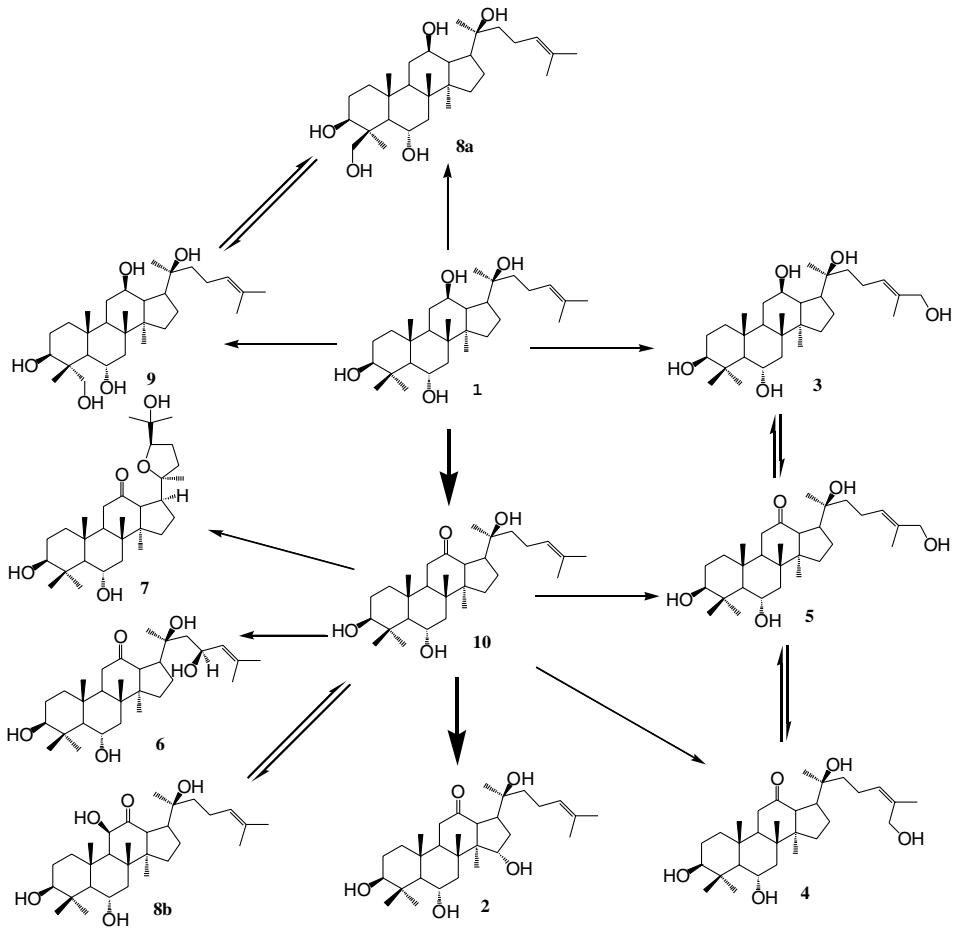

Fig. 5. A proposed biotransformation pathway of 20(*S*)-protopanaxatriol by *M. spinosus* AS 3.3450. Bold arrows indicate major transformation reactions.

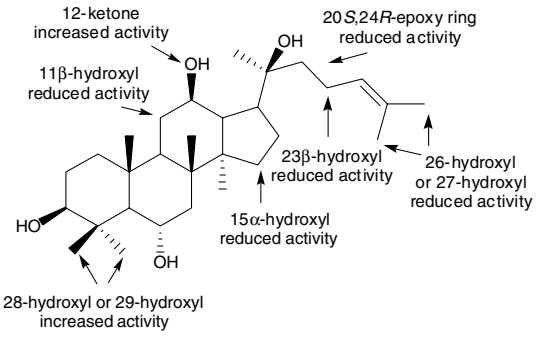

Fig. 6. Structure activity relationship of 20(*S*)-protopanaxatriol metabolites on growth inhibition of human leukemia HL-60 cells.

The importance of the 12-keto group for the cytotoxicity is in good agreement with previous reports (Atopkina et al., 1999). Metabolites **8a** and **9** were two active derivatives with hydroxylated methyl groups; however, most previous studies focused on hydroxylation in the ring and there was little previous research on the hydroxylation of the methyl group at C-28, C-29, C-26 and C-27 and their effects on the cytotoxicities. Therefore, this study is significant for the structure activity relationship research of ginsenosides (Fig. 6).

3. Concluding remarks

In conclusion, we provided a useful tool to prepare a variety of bioactive derivatives of 20(*S*)-protopanaxatriol (**1**) and to determine some important steps in its metabolism. The *in vitro* cytotoxicities of the metabolites suggested that 12-carbonylation or hydroxylation at C-28 or C-29 would increase the cytotoxic activities, whereas introduction of a hydroxyl group at C-11β, C-15α, C-23β, C-26 or C-27 would reduce the activity of the substrate. The metabolites **8a**, **9** and **10** had more potent cytotoxic activities against the HL-60 cell line compared with the substrate. Their potential as antitumor compounds warrants further investigation.

4. Experimental

4.1. General experimental procedures

Optical rotations were measured with a Perkin–Elmer 243B polarimeter in MeOH at 25 °C. IR spectra were determined in KBr with a Nicolet Avatar FT-IR spectrometer. 1D and 2D NMR spectra were recorded in pyridine-d_5 with a Varian INOVA 500 spectrometer using TMS as the internal standard. The chemical shifts were given in δ (ppm). HR-ESI-MS was performed using an ABI Qstar mass spectrometer. HPLC analyses were performed on an Agilent 1100 apparatus equipped with a diode-array detector and a quaternary pump system. The column was a YMC Pak ODS-A column (150 mm × 4.6 mm i.d.). For preparative HPLC, a TSP P100 pump connected to a TSP UV 100 detector and a YMC Pak ODS-A column (250 mm × 20 mm i.d.) was used. The mobile phase for analyses of the biotransformation products was linear gradient from CH_3CN–H_2O (30:70, v/v) to CH_3CN–H_2O (100:0, v/v) over 30 min, where it was held for 10 min. The flow rate was 0.7 ml/min for analysis and 2.0 ml/min for preparation. The detection wavelength was 203 nm and the column temperature was 25 °C. TLC was performed on pre-coated silica gel plates (Silica gel 60 F_{254}, Merck, Co. Germany). Column chromatography was performed on silica gel (200–300 mesh, Qingdao Marine Chemical Corporation, Qingdao, China).

4.2. Preparation of 20(S)-protopanaxatriol (1)

Ginseng extract was purchased from Jiuhui Co. Ltd. (Changsha, Hunan, China) and the total ginsenoside content was more than 80% (w/w). Ginseng extract powder (50 g) was oxidized with $NaIO_4$ (217 g) in H_2O (4000 ml) with stirring for 4 h 40 min. The mixture was filtered and washed with 2 N H_2SO_4 and then with H_2O. The precipitate was dissolved in 750 ml EtOH–H_2O (70:30, v/v), and $NaBH_4$ (17 g) was added. The solution was incubated for 17 h at room temperature. After dilution with water (750 ml), the pH of the solution was adjusted to 1.8–2.0 by adding 2 N H_2SO_4, and was then left overnight at room temperature. The reaction mixture was extracted with equal volume of EtOAc for three times and the organic layer was evaporated. The crude extract was subjected to a silica gel column and eluted with $CHCl_3$–EtOAc–EtOH (5:1:3 ratio, v/v–1:1:3 ratio, v/v) to produce **1** (2.1 g), which was identified by comparing its NMR spectroscopic data with previous reports in the literature (Asakawa et al., 1977). The purity of **1** was determined to be >98% by HPLC analysis.

4.3. Microorganisms and culture media

Mucor spinosus was purchased from the China General Microbiological Culture Collection Center in Beijing, China.

4.4. Biotransformation

Preliminary screenings were conducted in 250 ml Erlenmeyer flasks containing 100 ml of medium. The fungal mycelia were grown in shake cultures at 25 °C at 150 rpm. After 24 h, 2 mg of **1** (20 mg/ml) in MeOH was added to the cultures. Both substrate and organism controls were made. The incubation continued for a further 5 days. The cultures were then filtered and the filtrate extracted with EtOAc. Solvent was removed under vacuum, and the residue was dissolved in 1 ml of MeOH for analysis. The preparative experiments with *M. spinosus* AS 3.3450 were conducted in 1000 ml Erlenmeyer flasks

containing 400 ml of medium, which had been pre-cultured for 24 h. The substrate (800 mg) in MeOH (40 mg/ml) was evenly distributed among 40 flasks. The procedure and conditions were the same as for the preliminary experiments. The residue (1.98 g) obtained was applied to a silica gel column with $CHCl_3$–EtOAc–EtOH mixtures of increasing polarity, then purified by preparative HPLC (CH_3CN–H_2O) to produce **2** (57 mg), **3** (25 mg), **4** (20 mg), **5** (12 mg), **6** (9.6 mg), **7** (20 mg), **8a** (4.4 mg), **8b** (24 mg), **9** (15 mg) and **10** (54 mg).

4.4.1. 12-Oxo-23β-hydroxyl-20(S)-protopanaxatriol (6)

White amorphous powder; $[\alpha]_D^{25}$ +53.8 (MeOH; *c* 0.20); IR ν_{max}^{KBr} cm^{-1}: 3413 (–OH), 2970, 2933, 1699 (>C=O), 1385, 1037; HR-ESI-MS *m/z* $[M+Na]^+$ 513.3526 (calc. for $C_{30}H_{50}O_5Na$, 513.3556); ^1H and ^{13}C NMR, see Tables 1 and 2, respectively.

4.4.2. 20S,24R-Epoxy-dammaran-3β,6α,25-triol-12-one (7)

White amorphous powder; $[\alpha]_D^{25}$ +49.9 (MeOH; *c* 0.28); IR ν_{max}^{KBr} cm^{-1}: 3481 (–OH), 2969, 2931, 1707 (>C=O), 1384, 1085; HR-ESI-MS *m/z* $[M+Na]^+$ 513.3554 (calc. for $C_{30}H_{50}O_5Na$, 513.3558); ^1H and ^{13}C NMR, see Tables 1 and 2, respectively.

4.4.3. 29-Hydroxyl-20(S)-protopanaxatriol (8a)

White amorphous powder; $[\alpha]_D^{25}$ +44.0 (MeOH; *c* 0.10); IR ν_{max}^{KBr} cm^{-1}: 3382 (–OH), 2960, 2930, 1382, 1031; HR-ESI-MS *m/z* $[M+Na]^+$ 515.3717 (calc. for $C_{30}H_{52}O_5Na$, 515.3712); ^1H and ^{13}C NMR, see Tables 1 and 2, respectively.

4.4.4. 12-Oxo-11β-hydroxyl-20(S)-protopanaxatriol (8b)

White amorphous powder; $[\alpha]_D^{25}$ +40.7 (MeOH; *c* 0.29); IR ν_{max}^{KBr} cm^{-1}: 3430 (–OH), 2969, 2933, 1705 (>C=O), 1389, 1038; HR-ESI-MS *m/z* $[M+Na]^+$ 513.3546 (calc. for $C_{30}H_{50}O_5Na$, 513.3556); ^1H and ^{13}C NMR, see Tables 1 and 2, respectively.

4.4.5. 28-Hydroxyl-20(S)-protopanaxatriol (9)

White amorphous powder; $[\alpha]_D^{25}$ +39.1 (MeOH; *c* 0.41); IR ν_{max}^{KBr} cm^{-1}: 3308 (–OH), 2964, 2931, 1451, 1032; HR-ESI-MS *m/z* $[M+Na]^+$ 515.3707 (calc. for $C_{30}H_{52}O_5Na$, 515.3712); ^1H and ^{13}C NMR, see Tables 1 and 2, respectively.

Table 1
^1H NMR spectroscopic data for compounds **6**–**10** (pyridine-d_5, 500 MHz)

H	6	7	8a	8b	9	10
1	1.40 *m*	1.40 *m*	1.67 *m*	2.05 *m*	1.67 *m*	1.41 *m*
	0.94 *m*	0.93 *m*	1.03 *m*	1.26 *m*	1.05 *m*	0.94 *m*
2	1.88 *m*	1.88 *m*	2.01 *m*	2.10 *m*	1.97 *m*	1.86 *m*
	1.82 *m*	1.83 *m*	1.97 *m*	1.92 *m*	1.91 *m*	1.83 *m*
3	3.48 *m*	3.47 *m*	3.67 *m*	3.56 (*dd*, 4,12)	3.97 (*dd*, 5,11)	3.48 (*dd*, 5,11)
5	1.22 (*d*, 10.5)	1.21 (*d*, 10.5)	1.29 *m*	1.27 (*d*, 10)	1.60 *m*	1.22 (*d*, 10.5)
6	4.43 *m*	4.44 *m*	4.52 *m*	4.63 *m*	4.36 (*td*, 5,10)	4.43 *m*
7	1.93 (*dd*, 4.5,14)	1.91 *m*	1.94 (*d*, 10)	2.01 *m*	1.92 *m*	1.93 *m*
	1.90 (*dd*, 2,14)	1.86 *m*	1.88 (*dd*, 10)	1.96 *m*		1.92 *m*
9	1.88 *m*	1.84 *m*	1.57 *m*	1.69 *m*	1.61 *m*	1.88 *m*
11	2.37 (*dd*, 4.5,13)	2.33 *m*	2.14 *m*	4.75 (*t*, 3)	2.15 *m*	2.38 *m*
	2.30 *m*	2.31 *m*	1.52 *m*		1.54 *m*	2.30 *m*
13	3.31 (*d*, 9.5)	3.12 (*d*, 9.5)	2.03 *m*	4.41 (*d*, 9.5)	2.04 *m*	3.32 (*d*, 9.5)
15	1.85 *m*	1.78 *m*	1.52 *m*	2.11 *m*	1.60 *m*	1.85 *m*
	1.13 *m*	1.10 *m*	1.03 *m*	1.28 *m*	1.05 *m*	1.15 *m*
16	2.08 *m*	1.78 *m*	1.87 *m*	2.23 *m*	1.86 *m*	2.04 *m*
	1.84 *m*	1.76 *m*	1.36 *m*	1.93 *m*	1.38 *m*	1.85 *m*
17	2.63 *m*	2.72 *m*	2.31 *m*	2.88 (*td*, 4.5,10)	2.32 *m*	2.70 (*td*, 5.5,10)
18	1.27 (3H, *s*)	1.28 (3H, *s*)	1.08 (3H, *s*)	1.90 (3H, *s*)	1.10 (3H, *s*)	1.26 (3H, *s*)
19	0.99 (3H, *s*)	0.99 (3H, *s*)	1.05 (3H, *s*)	1.82 (3H, *s*)	1.01 (3H, *s*)	0.98 (3H, *s*)
21	1.56 (3H, *s*)	1.21 (3H, *s*)	1.40 (3H, *s*)	1.40 (3H, *s*)	1.41 (3H, *s*)	1.40 (3H, *s*)
22	2.17 (*dd*, 10,14)	1.91 *m*	2.03 *m*	1.84 *m*	2.03 *m*	1.76 *m*
	1.61 *m*	1.54 *m*	1.68 *m*	1.77 *m*	1.69 *m*	1.75 *m*
23	5.12 *m*	2.01 *m*	2.59 *m*	2.39 *m*	2.60 *m*	2.39 *m*
		1.91 *m*	2.27 *m*	2.26 *m*	2.28 *m*	2.27 *m*
24	5.52 (*d*, 8)	3.93 (*t*, 7)	5.31 (*t*, 7)	5.21 *m*	5.32 *m*	5.25 *m*
26	1.64 (3H, *s*)	1.39 (3H, *s*)	1.64 (3H, *s*)	1.62 (3H, *s*)	1.65 (3H, *s*)	1.64 (3H, *s*)
27	1.64 (3H, *s*)	1.35 (3H, *s*)	1.61 (3H, *s*)	1.58 (3H, *s*)	1.62 (3H, *s*)	1.59 (3H, *s*)
28	1.96 (3H, *s*)	1.94 (3H, *s*)	2.12 (3H, *s*)	2.00 (3H, *s*)	4.52 (*d*, 10.5)	1.95 (3H, *s*)
					4.41 (*d*, 10.5)	
29	1.42 (3H, *s*)	1.40 (3H, *s*)	4.58 (*dd*, 2.5,10)	1.51 (3H, *s*)	1.33 (3H, *s*)	1.42 (3H, *s*)
			4.42 (*dd*, 5,10)			
30	0.87 (3H, *s*)	0.82 (3H, *s*)	0.95 (3H, *s*)	0.95 (3H, *s*)	0.93 (3H, *s*)	0.88 (3H, *s*)

Table 2
^{13}C NMR spectroscopic data for compounds **6**–**10** (pyridine-d_5, 125 MHz)

C	6	7	8a	8b	9	10
1	38.9 *t*	38.9 *t*	39.1*t*	39.1 *t*	39.0 *t*	38.9 *t*
2	27.9 *t*	27.9 *t*	28.2*t*	28.0 *t*	27.3 *t*	27.9*t*
3	78.1 *d*	78.1 *d*	79.6 *d*	78.3 *d*	73.0 *d*	78.1 *d*
4	40.3*s*	40.3 *s*	44.4*s*	40.4 *s*	44.0 *s*	40.3 *s*
5	61.5 *d*	61.5 *d*	62.1 *d*	62.3 *d*	55.9 *d*	61.5 *d*
6	67.6 *d*	67.6 *d*	68.2 *d*	68.0 *d*	66.3 *d*	67.6 *d*
7	46.7 *t*	46.8*t*	46.6 *t*	48.7 *t*	46.8 *t*	46.7*t*
8	41.7*s*	41.6 *s*	41.2 *s*	42.6 *s*	40.5 *s*	41.6*s*
9	54.0 *d*	54.1 *d*	50.4 *d*	55.6 *d*	49.7 *d*	53.9 *d*
10	39.4 *s*	39.4*s*	39.3 *s*	40.7 *s*	38.8 *s*	39.4*s*
11	40.0 *t*	40.1 *t*	32.2*t*	77.5 *d*	31.9*t*	40.0*t*
12	211.6 *s*	210.4 *s*	71.0 *d*	211.7 *s*	70.7 *d*	211.7 *s*
13	55.9 *d*	56.9 *d*	48.3 *d*	51.9 *d*	47.9 *d*	56.2 *d*
14	55.5 *s*	55.6 *s*	51.6 *s*	55.8 *s*	51.4 *s*	55.5 *s*
15	31.9*t*	32.2 *t*	31.3 *t*	33.2*t*	31.1 *t*	31.9*t*
16	24.7*t*	25.1 *t*	26.8 *t*	24.5 *t*	26.6 *t*	24.5 *t*
17	45.6 *d*	43.1 *d*	54.8*d*	43.0 *d*	54.5*d*	44.0 *d*
18	17.4 *q*	17.2 *q*	17.5 *q*	19.8 *q*	16.7 *q*	17.4 *q*
19	17.3 *q*	17.3 *q*	17.6 *q*	20.3 *q*	17.6 *q*	17.2 *q*
20	74.3 *s*	85.3 *s*	73.0 *s*	73.5 *s*	72.7 *s*	73.2 *s*
21	26.5 *q*	25.1 *q*	27.0 *q*	25.4 *q*	26.8 *q*	26.5 *q*
22	46.4*t*	35.7 *t*	35.8 *t*	42.7 *t*	35.6 *t*	41.9 *t*
23	66.2 *d*	26.9 *d*	23.0 *t*	23.6 *t*	22.7 *t*	23.6 *t*
24	130.6 *d*	84.6 *d*	126.3 *d*	125.9 *d*	126.0 *d*	125.8 *d*
25	131.9 *s*	71.1 *s*	130.8 *s*	130.7 *s*	130.5 *s*	130.8 *s*
26	25.7 *q*	26.4 *q*	25.8 *q*	25.7 *q*	25.5 *q*	25.8 *q*
27	18.1 *q*	27.0 *q*	17.7 *q*	17.6 *q*	17.4 *q*	17.6 *q*
28	31.8 *q*	31.7 *q*	27.1 *q*	31.9 *q*	69.3*t*	31.7 *q*
29	16.4 *q*	16.4 *q*	64.0 *t*	16.4 *q*	13.3 *q*	16.4 *q*
30	17.1 *q*	16.8 *q*	17.0 *q*	17.2 *q*	16.8 *q*	17.2 *q*

4.4.6. 12-Oxo-20(S)-protopanaxatriol (*10*)

White amorphous powder; $[\alpha]_D^{25}$ +46.9 (MeOH; *c* 0.49); IR ν_{max}^{KBr} cm^{-1}: 3409 (–OH), 2970, 2931, 1695 (>C=O), 1385, 1036; HR-ESI-MS *m/z* $[M+Na]^+$ 497.3598 (calc. for $C_{30}H_{50}O_4Na$, 497.3607); ^1H and ^{13}C NMR, see Tables 1 and 2, respectively.

4.5. Time course investigation of biotransformation

The medium was identical to that used for screening-scale experiments. The fungus *M. spinosus* AS 3.3450 was transferred to the medium and incubated for 24 h, then 130 mg of **1** (5 mg for each flask) was added and the mixture was incubated for 3, 6, 9, 12, 24, 36, 48, 60, 72, 96, 120, 144 and 168 h. Mycelia were removed and the filtrate was treated as described above. The residue was dissolved in MeOH (1 ml), 10 μl of which was then analyzed by HPLC. All measurements were made in duplicate.

4.6. Bioassay

All the cell lines were maintained in RPMI 1640 medium (GIBCO/BRL, Maryland, USA) supplemented with 10% (v/v) fetal bovine serum, 100 IU/ml penicillin and 100 μg/ml streptomycin at 37 °C, 5% CO_2 and grown in 96-well microtiter plates for the assay. All compounds were dissolved in DMSO. After 24 h of incubation, compounds underwent in serial dilution to give final concentrations of 0.1–100 μg/ml. The cell growth was evaluated by the MTT assay (Sargent and Taylor, 1989). The activities were measured as IC_{50} values, that is, the concentration of test compound (μM) that inhibits cell growth by 50%.

Acknowledgement

We thank the Specialized Research Fund for the Doctoral Program of Higher Education (No. 20040001136) for financial support.

References

Asakawa, J., Kasai, R., Yamasaki, K., Tanaka, O., 1977. ^{13}C NMR study of Ginseng sapogenins and their related dammarane type triterpenes. Tetrahedron 33, 1935–1939.

Atopkina, L.N., Malinovskaya, G.V., Elyakov, G.B., Uvarova, N.L., Woerdenbag, H.J., 1999. Cytotoxicity of natural ginseng glycosides and semisynthetic analogues. Planta Med. 65, 30–34.

Bae, E.A., Han, M.J., Choo, M.K., Park, S.Y., Kim, D.H., 2002. Metabolism of 20(*S*)- and 20(*R*)-ginsenoside Rg3 by human intestinal bacteria and its relation to *in vitro* biological activities. Biol. Pharm. Bull. 25, 58–63.

de Carvalho, C.C.C.R., da Fonseca, M.M.R., 2006. Biotransformation of terpenes. Biotechnol. Adv. 24, 134–142.

Duc, N.M., Kasai, R., Ohtani, K., Ito, A., Nham, N.T., Yamasaki, K., Tanaka, O., 1994. Saponins from Vietnamese Ginseng, *Panax vietnamensis* Ha et Grushv collected in central Vietnam. III. Chem. Pharm. Bull. 42, 634–640.

Fujita, S., Kasai, R., Ohtani, K., Yamasaki, K., Ming-Hua, C., Rui-Lin, N., Tanaka, O., 1995a. Dammarane glycosides from aerial parts of *Neoalsomitra integrifoliola*. Phytochemistry 38, 465–472.

Fujita, S., Kasai, R., Ohtani, K., Yamasaki, K., Ming-Hua, C., Rui-Lin, N., Tanaka, O., 1995b. Dammarane glycosides from aerial part of *Neoalsomitra integrifolia*. Phytochemistry 39, 591–602.

Hasegawa, H., Sung, J.H., Matsumiya, S., Uchiyama, M., Inouye, Y., Kasai, R., Yamasaki, K., 1995. Reversal of daunomycin and vinblastine resistance in multidrug-resistant P388 Leukemia *in vitro* through enhanced cytotoxicity by triterpenoids. Planta Med. 61, 409–413.

Hasegawa, H., Suzuki, R., Nagaoka, T., Tezuka, Y., Kadota, S., Saiki, I., 2002. Prevention of growth and metastasis of murine melanoma through enhanced natural-killer cytotoxicity by fatty acid-conjugate of protopanaxatriol. Biol. Pharm. Bull. 25, 861–866.

Liu, Y., Li, W., Li, P., Deng, M.C., Yang, S.L., Yang, L., 2004. The inhibitory effect of intestinal bacterial metabolite of ginsenosides on CYP3A activity. Biol. Pharm. Bull. 27, 1555–1560.

Mochizuki, M., Yoo, Y.C., Samukawa, K., Matsuzawa, K., Sato, K., Saiki, I., Tono-oka, S., Samukawa, K., Azuma, I., 1995. Inhibitory effect of tumor metastasis in mice by saponins, ginsenoside-Rb2, 20(*R*)- and 20(*S*)-ginsenoside-Rg3, of Red ginseng. Biol. Pharm. Bull. 18, 1197–1202.

Nagai, M., Ando, T., Tanaka, N., Tanaka, O., Shibata, S., 1972. Chemical studies on the Oriental plant drugs XXVIII. Saponins and sapogenins of Ginseng. Stereochemistry of the sapogenin of Ginsenosides -Rb1, -Rb2, and Rc. Chem. Pharm. Bull. 20, 1212–1216.

Popovich, D.G., Kitts, D.D., 2002. Structure–function relationship exists for ginsenosides in reducing cell proliferation and inducing apoptosis in the human leukemia (THP-1) cell line. Arch. Biochem. Biophys. 406, 1–8.

Popovich, D.G., Kitts, D.D., 2004a. Mechanistic studies on protopanaxadiol, Rh2, and ginseng (*Panax quinquefolius*) extract induced cytotoxicity in intestinal Caco-2 cells. J. Biochem. Mol. Toxicol. 18, 143–149.

Popovich, D.G., Kitts, D.D., 2004b. Ginsenosides 20(*S*)-protopanaxadiol and Rh2 reduce cell proliferation and increase sub-G1 cells in two

cultured intestinal cell lines, Int-407 and Caco-2. Can. J. Physiol. Pharmcol. 82, 183–190.

Sargent, J.M., Taylor, C.G., 1989. Appraisal of the MTT assay as a rapid test of chemosensitivity in acute myeloid leukaemia. Br. J. Cancer 60, 206–210.

Sato, K., Mochizuki, M., Saiki, I., Yoo, Y.C., Samukawa, K., Azuma, I., 1994. Inhibition of tumor angiogenesis and metastasis by a saponin of *Panax ginseng*, ginsenoside-Rb2. Biol. Pharm. Bull. 17, 635–639.

Shibata, S.J., 2001. Chemistry and cancer preventing activities of ginseng saponins and some related triterpenoid compounds. Korean Med. Sci. 16 (Suppl.), S28–S37.

Shinkai, K., Akedo, H., Mukai, M., Imamura, F., Isoai, A., Kobayashi, M., Kitagawa, I., 1996. Inhibition of in vitro tumor cell invasion by ginsenoside Rg3. Jpn. J. Cancer Res. 87, 357–362.

Tian, Y., Guo, H., Han, J., Guo, D., 2005. Microbial transformation of 20(*S*)-protopanaxatriol by *Mucor spinosus*. J. Nat. Prod. 68, 678–680.

Wakabayashi, C., Hasegawa, H., Murata, J., Saiki, I., 1997. The expression of *in vivo* anti-metastatic effect of ginseng protopanaxatriol saponins is mediated by their intestinal bacterial metabolites after oral administration. Wakan Iyakugaku Zasshi 14, 180–185.